Simplified Configuration Design of Anthropomorphic Hand Imitating Specific Human Hand Grasps

Xinyang Tian, Qiang Zhan, Yin Zhang, Junyi Zou, Lingxiao Jiang, and Qinhuan Xu

***Abstract*—How to design an anthropomorphic hand imitating specific human hand grasps with as few actuators as possible is still a challenge. This letter presents a method for obtaining a simplified configuration of anthropomorphic hand imitating specific human hand grasps based on the motion analyses of the human hand. A participation matrix which characterizes a human hand grasp on joint motion level is constructed according to the motion participation of each finger joint. By adding all participation matrices of expected human hand grasps together a total participation matrix can be derived, and through mathematical processing a simplified anthropomorphic hand configuration can be obtained. Following the proposed method, a simplified anthropomorphic hand configuration that imitates six basic human hand grasps was obtained. A series of grasp experiments with the anthropomorphic hand prototype were conducted to validate the grasping capability as well as the proposed simplified configuration design method. This method can help to obtain a reasonably simplified configuration of an anthropomorphic hand when expected human hand grasps are definite.**

***Index Terms*—Anthropomorphic hand, configuration design, human hand grasp, participation matrix.**

I. Introduction

With increasing number of service robots being developed for personal and domestic use, ever more dexterous end-effectors and delicate manipulations are pursued [1]. Since most objects in human living environments are designed according to the structure and grasping characteristics of the human hand (cups, spoons, tools et al.), equipping service robots with anthropomorphic hands capable of proficient grasping is very beneficial for completing various tasks. In recent decades, lots of institutes and researchers focused on the design, control, manipulation of anthropomorphic hands, and many typical prototypes have been developed, such as Stanford/JPL hand [2], DLR-II hand [3], Shadow hand [4], and Schunk SVH hand [5], which have 9, 13, 20, and 9 degrees of freedom (DOFs), respectively. However, universal-type anthropomorphic hands use so many actuators to make them complex and expensive. Usually, an anthropomorphic hand is used to conduct certain tasks in a specific place, such as a house, a restaurant, or a workshop, where the human hand grasps to be replaced are known and finite. Therefore, anthropomorphic hands for specific applications have a wide range of needs. However, designing an anthropomorphic hand imitating specific human hand grasps with as few actuators as possible remains a problem.

The hand configuration should be formulated first when designing an anthropomorphic hand, because it determines both the hand structure and the number and distribution of fingers, joints, and active DOFs [6], [7]. However, little attention has been paid to the configuration design of anthropomorphic hands, and the most common approach to design the configuration of an anthropomorphic hand is using experience together with grasping simulations. For example, the configurations of SmartHand [8] and DLR/HIT hand [9] were first obtained based on real-life experiences, and then optimized through simulation and experimentation. While this procedure improves the configuration sequentially, it is expensive and does not necessarily produce an optimal configuration. Due to the complexity of configuration design, local optimization strategies are sometimes used to obtain a reasonable configuration of a single finger, especially the thumb. Wang et al. [10] proposed an evaluation method based on kinetostatic and dynamic dexterity as well as the workspace to improve the configuration rationality of an anthropomorphic thumb, but it was not applied to the configuration design of a whole hand. You et al. [11] presented a "interactivity of fingers" performance index to optimize an anthropomorphic hand, but it can only determine the position and orientation of the saddle joint of the thumb. Most current research mainly focuses on studying actuator arrangement and drive transmission mechanism [12], [13], [14] based on existing configurations, and rarely on designing corresponding configurations for specific applications.

Besides, describing human hand grasps mathematically is also vital for deciding the configuration of an anthropomorphic hand imitating human hand grasps. Xiong et al. [15] studied the movement relationship among the postural synergic characteristics of human hand fingers, and proposed a hand function evaluation model that can establish the relationship between morphological structure and operational functions. This method was evaluated by the X-hand, but it mainly focused on the postural synergic characteristics of fingers and structure design, not the configuration design. Kang et al. [16] described different grasps of the human hand using a contact network containing contact points; however, it does not accurately reflect the grasping characteristics of the thumb. Liu et al. [17] described the human hand grasps using VF (Virtual Finger) tree graph by dividing the thumb into an independent region. However, as the same finger-object contact may correspond to different joint motions, there may exist multiple solutions for configuration design.

Manuscript received 29 July 2022; accepted 14 November 2022. Date of publication 23 November 2022; date of current version 29 November 2022. This letter was recommended for publication by Associate Editor M. Dogar and Editor H. Liu upon evaluation of the reviewers' comments. *(Corresponding author: Qiang Zhan.)*

Xinyang Tian, Qiang Zhan, Junyi Zou, Lingxiao Jiang, and Qinhuan Xu are with the Robotics Institute of Beihang University, Beijing 100191, China (e-mail: tianers@buaa.edu.cn; qzhan@buaa.edu.cn; 16071014@buaa.edu.cn; xjling@buaa.edu.cn; xuqinhuan@buaa.edu.cn).

Yin Zhang is with the Beijing Electro-Mechanical Engineering Institute, Beijing 100074, China (e-mail: zhangyin9013@163.com).

Digital Object Identifier 10.1109/LRA.2022.3224309

In summary, there is still a lack of effective method for the configuration design of anthropomorphic hands imitating specific human hand grasps. To address this problem, this letter presents a simplified configuration design method based on finger joint participation of the human hand. The main contribution of this letter is providing a method for obtaining the configuration of an anthropomorphic hand imitating specific human hand grasps with as few actuators as possible.

The remainder of this letter is organized as follows. In Section II analyzes the motion characteristics of the human hand, and presents its configuration. Section III introduces a mathematical description method for human hand grasps. Section IV presents a configuration simplification method of anthropomorphic hands. Section V offer an example of the simplified configuration design of an anthropomorphic hand imitating six basic human hand grasps, and its prototype validation is given in Section VI. The concluding remarks are given in Section VII.

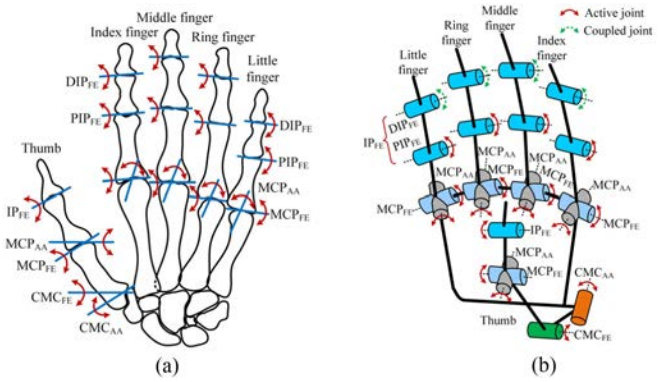

Fig. 1. (a) Mechanism sketch of the human hand. (b) The equivalent configuration of the human hand.

II. Configuration of the Human Hand

The human hand is a complex biological system comprising bones, joints and tissues [18]. From a structural perspective, it can be divided into two main parts: the palm and the fingers. The fingers can be further divided into a thumb with a unique structure and other four fingers with similar structure.

The palm consists of five metacarpals connected to a thumb and four fingers respectively. The joints between metacarpals and carpal bones are called carpometacarpal (CMC) joints. The CMC joint of the thumb has a large range of motion, while the CMC joints of other four fingers have a more limited range [19]. Since actuators, controllers and sensors are often mounted inside the palm, it is usually used as the basis of an anthropomorphic hand.

As the most important finger of the human hand the thumb is mainly composed of a trapezium, a metacarpal, a proximal phalanx, a distal phalanx, a metacarpophalangeal (MCP) joint, an interphalangeal (IP) joint, and a CMC joint. At present, there is no consensus on the motion principle of the CMC joint of the thumb, but it is more inclined to think that it is a saddle joint with two non-orthogonal and non-intersecting motion axes, and the flexion/extension axis is at the distal end of the carpal bone while the abduction/adduction axis is at the base of the metacarpal [20]. Therefore, the CMC joint of the thumb has two DOFs. The MCP joint between the metacarpal and the proximal phalanx is an ellipsoidal joint that allows both flexion/extension and abduction/adduction motions. The axes of these two motions are approximately orthogonal and intersected. The IP joint between the proximal phalanx and the distal phalanx is a rotation joint that allows a flexion/extension motion. Therefore, the thumb is equivalent to a 5 DOFs mechanism with three joints. Its motions mainly comprise the abduction/adduction and flexion/extension motions of the CMC joint, the abduction/adduction and the flexion/extension motions of the MCP joint and the flexion/extension motion of the IP joint. For convenience, these motions are denoted as $\mathrm{CMC_{AA}}$, $\mathrm{CMC_{FE}}$, $\mathrm{MCP_{FE}}$, $\mathrm{MCP_{AA}}$, and $\mathrm{IP_{FE}}$, respectively.

The other four fingers share a similar structure, which comprises a metacarpal, a proximal phalanx, a middle phalanx, and a distal phalanx. Their MCP joints all allow flexion/extension motion and abduction/adduction motion. Both their proximal interphalangeal (PIP) joints and distal interphalangeal (DIP) joints allow flexion/extension motions, and the two flexion/extension axes of each finger are approximately parallel [19]. Therefore, each finger is equivalent to a 4 DOFs mechanism with three joints. Their motions mainly include the flexion/extension and abduction/adduction motions of the MCP joint, the flexion/extension motions of the PIP joint and the DIP joint. For convenience, these motions are denoted as $\mathrm{MCP_{FE}}$, $\mathrm{MCP_{AA}}$, $\mathrm{PIP_{FE}}$, and $\mathrm{DIP_{FE}}$, respectively.

Therefore, the human hand is equivalent to a 21 DOFs mechanism with fifteen joints, and its mechanism sketch is illustrated in Fig. 1(a), where the blue lines denote the approximate locations of motion axes, and the arrows denote joint rotations around corresponding axes.

III. Description of Human Hand Grasps

The Human hand can perform various grasps through the coordinated motions of different fingers, which are essentially realized by the coordination of different joint motions. Therefore, joint motion is the most basic motion component of the human hand. Accordingly, we propose to use an index of "joint participation" to describe whether a joint motion is involved in a specific static grasp. This could be denoted as $(a_i^j)_k$, where, i denotes the type of a joint motion, $i \in \{\mathrm{CMC_{AA}}, \mathrm{CMC_{FE}}, \mathrm{MCP_{FE}}, \mathrm{MCP_{AA}}$ and $\mathrm{IP_{FE}}\}$; j denotes the name of a finger, $j \in \{T, I, M, R, L\}$ (where T, I, M, R and L denote the thumb, the index finger, the middle finger, the ring finger, and the little finger, respectively); k denotes the type of a human hand grasp. When finger j is involved in a grasp, $(a_i^j)_k$ can be expressed as:

$$(a_i^j)_k = \frac{\left|(\theta_i^j)_k\right|}{m_i}, 0 \le \left|(\theta_i^j)_k\right| \le m_i \tag{1}$$

Where, $(\theta_i^j)_k$ denotes the rotation angle of joint j from an initial fully expanded posture to grasping posture in grasp k, m_i denotes the maximum rotation angle of joint motion i depending on the joint motion type, when the joint motion is FE $m_i = 90^\circ$, when the joint motion is AA $m_i = 30^\circ$, according to the study of human hand anatomy [18], [19].

According to the motion analysis of the human hand, some assumptions are listed as follows:

1) In most grasping cases, the $\mathrm{PIP_{FE}}$ motion and the $\mathrm{DIP_{FE}}$ motion are coupled. There are still some exceptions where these two joints move independently, such as fingertip grasp, hook grasp. However, experience shows that these

two grasps can be completed even if the $\mathrm{DIP_{FE}}$ motion does not participate in them. Hence, the $\mathrm{DIP_{FE}}$ motion and the $\mathrm{PIP_{FE}}$ motion could be coupled and represented by one $\mathrm{IP_{FE}}$ motion, i.e., using $\mathrm{IP_{FE}}$ to denote $\mathrm{PIP_{FE}}$ and $\mathrm{DIP_{FE}}$ for each finger.

2) Opposition of the thumb comes from the combined motion of all its joints. Therefore, when grasp involves the opposition of the thumb, it can be assumed that all joint motions of the thumb participate in it. Moreover, the two motion axes of the CMC joint of the thumb are assumed to be orthogonal.
3) During a grasp, some fingers contact with an object may cause other fingers to move due to skin or personal habits. However, the joint motions of the passively moved fingers are not necessary for finishing the grasp. Therefore, the joint motions of the passively fingers unnecessary to a given grasp are disregarded.

On the basis of the above the equivalent configuration of the human hand is obtained, as shown in Fig. 1(b), which has 17 DOFs.

Based on the joint participation $(a_i^j)_k$ and the above assumptions, a joint participation matrix $\boldsymbol{P}_k \in \mathbb{R}^{5\times5}$ is defined to characterize a human hand grasp k from the joint level, as shown in (2) shown at the bottom of this page. In matrix $\boldsymbol{P}_k$, each row represents a finger, from the first to last are the thumb, the index finger, the middle finger, the ring finger, and the little finger, respectively. The elements from the first to the last of each row are $\mathrm{CMC_{AA}}$, $\mathrm{CMC_{FE}}$, $\mathrm{MCP_{FE}}$, $\mathrm{MCP_{AA}}$, and $\mathrm{IP_{FE}}$, respectively.

Matrix $\boldsymbol{P}_k$ denotes the participation of each joint motion in a single grasp. When different grasps need considering together, the matrix $\boldsymbol{P}_k$ corresponding to each grasp can be added together using (3):

$$\boldsymbol{P} = [p_{ij}]_{5\times5} = \sum \boldsymbol{P}_k \tag{3}$$

Where, $\boldsymbol{P}$ denotes the total joint participation matrix, p_{ij} denotes the total participation of joint motion i of finger j. The larger p_{ij}, the higher the corresponding joint participation.

Therefore, when designing an anthropomorphic hand, if the human hand grasps to be imitated are known, (3) can be used to derive all the necessary joint contributions of each finger. Thus, matrix $\boldsymbol{P}$ can represent the configuration of an anthropomorphic hand from a mathematical standpoint.

IV. Configuration Simplification Method

If the configuration derived from (3) is directly used to design an anthropomorphic hand, its structure will be complex and expensive. Therefore, it is necessary to simplify the configuration reasonably. According to matrix norm theory, the proximity of two identical dimension matrices can be evaluated by the norm of their difference matrix, which can be used to simplify matrix $\boldsymbol{P}$. Accordingly, one mapping and one criterion are defined as follows.

Mapping $\boldsymbol{f}$: $\boldsymbol{P} \to \boldsymbol{P}^r$, $\boldsymbol{P}^r = f(\boldsymbol{P}, r) = [p_{ij}']_{5\times5}$, $1 \le r \le n$, if $p_{ij} > r$, then $p_{ij}' = p_{ij}$, else $p_{ij}' = 0$. Where, n is the number of human hand grasps to be imitated; r is a positive integer starting from 1 and adding 1 per loop. Using mapping f, elements of matrix $\boldsymbol{P}^r$ less than or equal to r can be converted to 0 and the others remain unchanged.

Criterion $\boldsymbol{h}$: if $D(\tilde{p}_{ij}) > D$ or $\max(\tilde{p}_{ij}) < \lambda n$, $h = 1$, else $h = 0$. Where, $\tilde{p}_{ij}$ denotes a non-zero element in matrix $\boldsymbol{P}^{r-1}$; $\max(\tilde{p}_{ij})$ and $D(\tilde{p}_{ij})$ denote the maximum value and the maximum variance of all elements $\tilde{p}_{ij}$ respectively; λ represents a coefficient between joint participation and the number of human hand grasps, which can be determined according to the ratio of the number of expected human hand grasps and the number of total daily human hand grasps. Criterion h is mainly used to evaluate the participation differences among joint motions.

Subsequently, the target matrix $\boldsymbol{P}_E$ and the number of required actuators can be derived from matrix $\boldsymbol{P}$ based on matrix norm theory and the differences among matrix elements, and the specific processes are shown in Algorithm 1. ε is the allowed maximum relative deviation of two related matrix spectral norms, ξ is the expected coefficient given in advance, which is often equal to λ. $NOA\,((p_s^i)_E)$ denotes the number of required actuators for $(p_s^i)_E$, where s denotes the joint motion types and $s = \{\mathrm{FE}, \mathrm{AA}\}$, FE is the flexion/extension motion and AA is the abduction/adduction motion. Thus, $(p_s^i)_E$ denotes the motion type of each finger in matrix $\boldsymbol{P}_E$. The symbol $\|\ \|_2$ denotes the spectral norm. $\tilde{p}^{r-1}$ and $(\tilde{p}^{r-1})_q$ denote non-zero elements in matrix $\boldsymbol{P}^{r-1}$ and matrix $(\boldsymbol{P}^{r-1})_q$ respectively, and matrix $(\boldsymbol{P}^{r-1})_q$ is obtained from matrix $\boldsymbol{P}^{r-1}$ and q denotes the coupling mode among adjacent fingers. For example, $L{\to}R$ denotes the case that the 5th and the 4th rows of matrix $\boldsymbol{P}^{r-1}$ are added as the new 4th row, and the elements of the new 5th row are all set to be 0; $L{\to}R$ and $M{\to}I$ denote the case that the 5th and the 4th rows of matrix $\boldsymbol{P}^{r-1}$ are added as the new 4th row, and the 3rd and the 2nd rows of matrix $\boldsymbol{P}^{r-1}$ are added as the new 2nd row, then the elements of the 5th and the 3rd rows are all set to be 0. $\mathrm{num}(\min D((\tilde{p}^{r-1})_q))$ denotes the number of the minimal variance $\min D((\tilde{p}^{r-1})_q)$ related to matrix $(\boldsymbol{P}^{r-1})_q$, $\boldsymbol{P}^{r-1}_{\mathrm{q}\ (\min D(\tilde{p}_{ij}^{r-1})_q))}$ denotes the matrix with the minimal variance, and $\boldsymbol{P}^{r-1}{}^{(\max\|\tilde{p}_{ij}^{r-1}\|_2)}_{q\quad(\min D(\tilde{p}_{ij}^{r-1})_q))}$ denotes the matrix that has the minimal variance same to others, but it has the maximum spectral norm compared to other matrices, $E((\tilde{p}_s^i)_E)$ denotes the average of the non-zero participation $(\tilde{p}_s^i)_E$, and INT denotes an integer-valued function.

D, λ, ε and ξ are the decisive parameters. The bigger λ and ξ the smaller D and ε are, more easily the obtained configuration finishes the expected human hand grasps, but the corresponding complexity will increase. Therefore, those parameters need to be reasonably selected according to the specific requirements.

In short, Algorithm 1 contains three main steps: Step 1 removes joint motions with low participation; Step 2 couples joints to get $\boldsymbol{P}_E$; Step 3 distributes active DOFs to fingers.

$$\boldsymbol{P}_k = \left[(a_i^j)_k\right]_{5\times5} = \begin{bmatrix} (a^T_{CMC_{AA}})_k & (a^T_{CMC_{FE}})_k & (a^T_{MCP_{FE}})_k & (a^T_{MCP_{AA}})_k & (a^T_{IP_{FE}})_k \\ (a^I_{CMC_{AA}})_k & (a^I_{CMC_{FE}})_k & (a^I_{MCP_{FE}})_k & (a^I_{MCP_{AA}})_k & (a^I_{IP_{FE}})_k \\ (a^M_{CMC_{AA}})_k & (a^M_{CMC_{FE}})_k & (a^M_{MCP_{FE}})_k & (a^M_{MCP_{AA}})_k & (a^M_{IP_{FE}})_k \\ (a^R_{CMC_{AA}})_k & (a^R_{CMC_{FE}})_k & (a^R_{MCP_{FE}})_k & (a^R_{MCP_{AA}})_k & (a^R_{IP_{FE}})_k \\ (a^L_{CMC_{AA}})_k & (a^L_{CMC_{FE}})_k & (a^L_{MCP_{FE}})_k & (a^L_{MCP_{AA}})_k & (a^L_{IP_{FE}})_k \end{bmatrix}_{5\times5} \tag{2}$$

Algorithm 1: Tree Construction.

Input: $\boldsymbol{P}, n, \varepsilon, \lambda, {}_D, \xi, w_k$
Output: $\boldsymbol{P}_E$, $NOA((p_s^i)_E)$
1. **for** $r = 1; r \le n; r$++ **do**
2. Calculating $\boldsymbol{P}^r$ by mapping f and $\varepsilon_r = \|\boldsymbol{P} - \boldsymbol{P}^r\|_2 / \|\boldsymbol{P}\|_2$
3. **if** $\varepsilon_r < \varepsilon$ **then**
4. **repeat**
5. **end**
6. **end**
7. Calculating $\max(\tilde{p}_{ij})$ and $D(\tilde{p}_{ij})$ of P^{r-1}
8. **if** $h = 0$ **then**
9. $\boldsymbol{P}_E = \boldsymbol{P}^{r-1}$
10. **else**
11. Calculating $\boldsymbol{P}_q^{r-1}, q = \{L \to R; M \to I; L \to R; M \to I; L \to R \to M; L \to R \to M \to I\}$
12. Calculating $D((\tilde{p}_{ij}^{r-1})_q)$ and $num(\min D(\tilde{p}_{ij}^{r-1})_q)$
13. **end**
14. **if** $num(\min D(\tilde{p}_{ij}^{r-1})_q) = 1$ **then**
15. $\boldsymbol{P}_{q\ (\min D(\tilde{p}_{ij}^{r-1})_q)}^{r-1}$
16. **else**
17. $\boldsymbol{P}_E = \boldsymbol{P}_{q\ (\min D(\tilde{p}_{ij}^{r-1})_q)}^{r-1(\max\|p_q^{r-1}\|_2)}$
18. **end**
19. Calculating $(p_s^i)_E, i = \{T, I, M, R, L\}, s = \{\mathrm{FE}, \mathrm{AA}\}$
20. Calculating $NOA((\tilde{p}_s^i)_E) = INT((\tilde{p}_s^i)_E) / (\xi \cdot E((\tilde{p}_s^i)_E))$

Step 1 simplifies $\boldsymbol{P}$ as far as possible until $\|\boldsymbol{P} - \boldsymbol{P}^r\|_2 / \|\boldsymbol{P}\|_2 > \varepsilon$ by increasing r, then evaluates whether $\boldsymbol{P}^{r-1}$ matches h criterion.
Step 2 first tries to zero clearing specific rows of $\boldsymbol{P}^{r-1}$ and adds them to other rows, so there are different $(\boldsymbol{P}^{r-1})_q$ for different q, then chooses the optimal $(\boldsymbol{P}^{r-1})_q$ with $\min D((\tilde{p}^{r-1})_q)$ and maximal $\|(\tilde{p}^{r-1})_q\|_2$ as $\boldsymbol{P}_E$ in sequence. As a result, the non-zero elements in matrix $\boldsymbol{P}_E$ have smaller differences, Which means remaining joints have similar distribution in predetermined grasps.
Step 3 combines the same joint motion of each finger in matrix $\boldsymbol{P}_E$ to get the total FE/AA participation matrix $((p_s^i)_E)_{5\times 2}$. Finally, the number of the total FE/AA DOFs of each finger is obtained using $INT((p_s^i)_E)/\xi E((\tilde{p}_s^i)_E)$.

The proposed method can guide the formulation of the design criteria for anthropomorphic hands, through first obtaining the simplest configuration according to expected human hand grasps, then reasonably increasing or decreasing the number of joints and active DOFs in combination with personalization, fault tolerance and other factors, so as to formulate the final design criteria without involving structure design, actuator type and arrangement.

Furthermore, compared with synergistic-based approach [15], [21], the proposed method can not only simplify the number of joints and active DOFs of an anthropomorphic hand, but also exhibit more flexibility in realizing non-predetermined grasps.

V. Simplified Configuration Design of an Anthropomorphic Hand

Taylor and Schwarz summarized the main daily manipulations of the human hand into six basic grasps, i.e., cylindrical grasp, tip grasp, hook grasp, palmar grasp, spherical grasp, and lateral grasp [22]. These six basic grasps cover most of the human hand grasps in daily life, and many complex grasps can be seen as the combinations of them. Therefore, we choose the configuration design of an anthropomorphic hand that imitates the six basic human hand grasps as an example to verify the proposed method.

Fig. 2. Human hand motion acquisition system based on Leap Motion.

TABLE I
Cylindrical Grasp Examples and Joint Participation Matrix

Typical cylindrical grasp examples	$\boldsymbol{P}_{\text{cylindrical}}$
(a) (b) (c)	$\begin{bmatrix} 1 & 0 & 0.11 & 0 & 0.57 \\ 0 & 0 & 0.37 & 0 & 0.58 \\ 0 & 0 & 0.37 & 0 & 0.56 \\ 0 & 0 & 0.36 & 0 & 0.64 \\ 0 & 0 & 0.32 & 0 & 0.56 \end{bmatrix}$

(a) grasping a cup, (b) grasping a bottle, (c) grasping a drill.

A. Joint Motion Analyses and Participation Matrices of Six Human Hand Grasps

In order to identify the joint participation matrix of the six basic human hand grasps, an experimental system was built based on a previous device [23], as shown in Fig. 2. For each type of grasp, three objects of similar shape are selected to obtain the corresponding joint participation matrix, and the average value of fifteen experiments is taken as the final result of the matrix.

1) Cylindrical Grasp: The cylindrical grasp is mainly suitable for grasping cylindrical objects, and objects with different sizes can be grasped through the opposition of the thumb and the flexion motions of other four fingers. Though the MCP joints of other four fingers have slight abduction/adduction motions, they are small and can be ignored. Thus, the joint motions involved in cylindrical grasp are $\mathrm{CMC_{AA}}$, $\mathrm{CMC_{FE}}$, $\mathrm{MCP_{FE}}$, $\mathrm{MCP_{AA}}$ and $\mathrm{IP_{FE}}$ of the thumb along with $\mathrm{MCP_{FE}}$ and $\mathrm{IP_{FE}}$ of the other four fingers. Three typical cylindrical grasp examples and the corresponding joint participation matrix are shown in Table I.

2) Tip Grasp: The tip grasp is mainly suitable for grasping small objects. It is mainly achieved by the opposition of the thumb along with the flexion motion of the index finger (with 2-fingertips). The joint motions involved in tip grasp are $\mathrm{CMC_{AA}}$, $\mathrm{CMC_{FE}}$, $\mathrm{MCP_{FE}}$, $\mathrm{MCP_{AA}}$ and $\mathrm{IP_{FE}}$ of the thumb and $\mathrm{MCP_{FE}}$ and $\mathrm{IP_{FE}}$ of the index finger. Three typical tip grasp examples and the corresponding joint participation matrix are shown in Table II.

TABLE II
TIP GRASP EXAMPLES AND JOINT PARTICIPATION MATRIX

Typical tip grasp examples	$\boldsymbol{P}_{\text{tip}}$
 (a) grasping a strawberry, (b) grasping a screw, (c) rotating a switch.	$\begin{bmatrix} 1 & 0 & 0.03 & 0 & 0.89 \\ 0 & 0 & 0.47 & 0.10 & 0.57 \\ 0 & 0 & 0 & 0 & 0 \\ 0 & 0 & 0 & 0 & 0 \\ 0 & 0 & 0 & 0 & 0 \end{bmatrix}$

TABLE III
HOOK GRASP EXAMPLES AND JOINT PARTICIPATION MATRIX

Typical hook grasp examples	$\boldsymbol{P}_{\text{hook}}$
 (a) grasping a suitcase, (b) grasping a bucket, (c) grasping a handbag.	$\begin{bmatrix} 0 & 0 & 0 & 0 & 0 \\ 0 & 0 & 0.48 & 0 & 0.96 \\ 0 & 0 & 0.72 & 0 & 1 \\ 0 & 0 & 0.64 & 0 & 1 \\ 0 & 0 & 0.52 & 0 & 1 \end{bmatrix}$

TABLE IV
PALMAR GRASP EXAMPLES AND JOINT PARTICIPATION MATRIX

Typical palmar grasp examples	$\boldsymbol{P}_{\text{palmar}}$
 (a) grasping a pen, (b) grasping a screwdriver, (c) grasping a tweezer.	$\begin{bmatrix} 1 & 0 & 0.03 & 0.13 & 0.60 \\ 0 & 0 & 0.67 & 0 & 0.38 \\ 0 & 0 & 0.79 & 0 & 0.16 \\ 0 & 0 & 0 & 0 & 0 \\ 0 & 0 & 0 & 0 & 0 \end{bmatrix}$

3) Hook Grasp: The hook grasp is mainly suitable for picking up objects with handles. Its main feature is applying a force opposite to gravity by the flexion motions of four fingers. Thus, joint motions involved in a hook grasp are MCP_{FE} and IP_{FE} of four fingers. Three typical hook grasp examples and the corresponding joint participation matrix are shown in Table III.

4) Palmar Grasp: The palmar grasp is suitable for grasping slender objects. It is mainly achieved by the opposition of the thumb along with the flexion motions of the index finger and the middle finger. Therefore, the joint motions involved in a palmar grasp are CMC_{AA}, CMC_{FE}, MCP_{FE}, MCP_{AA} and IP_{FE} of the thumb along with MCP_{FE} and IP_{FE} of the index finger and the middle finger. Three typical palmar grasp examples and the corresponding joint participation matrix are shown in Table IV.

5) Spherical Grasp: The spherical grasp is suitable for grasping round objects. In this grasp the fingertips of the human hand are approximately distributed on one circle through the opposition of the thumb along with the flexion motions of other four fingers. To enhance the grasp stability, the abduction/adduction motions of the MCP joints of the index finger, the ring finger, and the little finger are also involved. Therefore, joint motions involved in spherical grasp are CMC_{AA}, CMC_{FE}, MCP_{FE}, MCP_{AA} and IP_{FE} of the thumb, MCP_{FE} and IP_{FE} of other four fingers, and MCP_{AA} of the index finger, the ring finger and the little finger. Three typical spherical grasp examples and the corresponding joint participation matrix are shown in Table V.

6) Lateral Grasp: The lateral grasp is suitable for grasping flat objects. It is mainly achieved by the opposition of the thumb along with the flexion motion of the index finger. Therefore, the joint motions involved in a lateral grasp are CMC_{AA}, CMC_{FE}, MCP_{FE}, MCP_{AA} and IP_{FE} of the thumb along with MCP_{FE} and IP_{FE} of the index finger. Three typical lateral grasp examples and the corresponding joint participation matrix are shown in Table VI.

TABLE V
SPHERICAL GRASP EXAMPLES AND JOINT PARTICIPATION MATRIX

Typical spherical grasp examples	$\boldsymbol{P}_{\text{spherical}}$
 (a) grasping an apple, (b) grasping a tennis, (c) grasping a Rubik's cube.	$\begin{bmatrix} 1 & 0 & 0.02 & 0.50 & 0.64 \\ 0 & 0 & 0.33 & 0.62 & 0.39 \\ 0 & 0 & 0.19 & 0 & 0.37 \\ 0 & 0 & 0.13 & 0.70 & 0.44 \\ 0 & 0 & 0.17 & 0.67 & 0.19 \end{bmatrix}$

TABLE VI
LATERAL GRASP EXAMPLES AND JOINT PARTICIPATION MATRIX

Typical lateral examples	$\boldsymbol{P}_{\text{lateral}}$
 (a) grasping a key, (b) grasping a USB, (c) grasping a card.	$\begin{bmatrix} 1 & 0 & 0 & 0.13 & 0.70 \\ 0 & 0 & 0.47 & 0 & 0.41 \\ 0 & 0 & 0 & 0 & 0 \\ 0 & 0 & 0 & 0 & 0 \\ 0 & 0 & 0 & 0 & 0 \end{bmatrix}$

TABLE VII
ACTIVE DOF DISTRIBUTION OF EACH FINGER

	$(p^i{}_s)_E$		$NOA((p^i{}_s)_E)$	
	FE	AA	FE	AA
T	3.40	5.00	1	1
I	6.07	0	1	0
M	4.15	0	1	0
R	5.97	0	1	0
L	0	0	0	0

Note that due to the motion of CMC_{FE} of the thumb is difficult to measure and can be replaced by MCP_{FE}, the element $\boldsymbol{P}_k(1, 2)$, of all six basic matrices are set to zero. Then, the joint participation matrix $\boldsymbol{P}_k$ corresponding to each basic grasp is added together to obtain the total joint participation matrix $\boldsymbol{P}$, as shown below.

$$\begin{aligned} \boldsymbol{P} &= \sum \boldsymbol{P}_k = \boldsymbol{P}_{\text{cylindrical}} + \boldsymbol{P}_{\text{tip}} + \boldsymbol{P}_{\text{hook}} + \boldsymbol{P}_{\text{palmar}} \\ &\quad + \boldsymbol{P}_{\text{spherical}} + \boldsymbol{P}_{\text{lateral}} \\ &= \begin{bmatrix} 5.00 & 0 & 0.20 & 0.75 & 3.40 \\ 0 & 0 & 2.78 & 0.73 & 3.29 \\ 0 & 0 & 2.07 & 0 & 2.08 \\ 0 & 0 & 1.13 & 0.70 & 2.09 \\ 0 & 0 & 1.01 & 0.65 & 1.74 \end{bmatrix} \end{aligned} \tag{4}$$

Matrix $\boldsymbol{P}$ in (4) shows that except MCP_{AA} of the middle finger, other joints of the human hand are all involved in the six basic grasps. However, their specific participation degrees are different. The joint participation degrees of the thumb, the index finger, the middle finger, the ring finger, and the little finger account for 33.8%, 24.6%, 15.0%, 14.2%, and 12.4% of the total joint motions, respectively. It indicates that the joint participation of the thumb is maximal. Besides, the joint participation of the index finger is about twice that of the ring finger, and the little finger and the ring finger have the same joint participation.

According to matrix $\boldsymbol{P}$ in (4), the expected anthropomorphic hand configuration that imitates the six basic hand

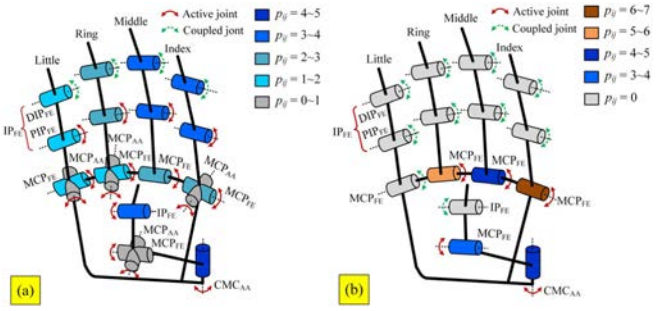

Fig. 3. Human hand configuration. (a) Hand configuration for six basic grasps (15 DOFs). (b) Simplified anthropomorphic hand configuration (5 DOFs).

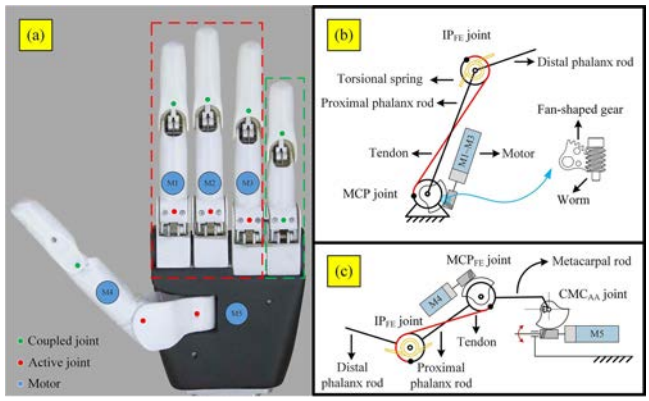

Fig. 4. (a) CMIC-5 hand prototype. (b) Actuation mechanism of fingers. (c) Actuation mechanism of the CMC$_{\mathrm{AA}}$ joint of the thumb.

grasps can be obtained, as shown in Fig. 3(a). The total DOF number of the configuration is 15. Where, the thumb, the index finger, the middle finger, the ring finger, and the little finger have 4, 3, 2, 3, and 3 DOFs, respectively. Obviously, the obtained anthropomorphic hand configuration is still complex. Therefore, it should be simplified reasonably.

B. The Simplified Anthropomorphic Hand Configuration

In this section, Algorithm 1 is used to simplify the anthropomorphic hand configuration, as shown in Fig. 3(a).

Related parameters are identified according to the design requirements: since the value of $\tilde{p}_{ij}$ is between 0 and 1, thus $D = 1$; six basic human hand grasps can cover about 70%∼90% of daily manipulations [22], thus $\lambda = \xi = 0.7$; according to the definition of λ and ξ, the value of ε cannot be too large, otherwise it will greatly increase the configuration complexity, thus the final value of ε is set as 0.2∼0.3 by experience. It is obvious that $n = 6$. Through the first "*for*" loop of Algorithm 1, the relative deviations between the total joint participation matrix and the corresponding transformation matrices can be calculated using MATLAB, where, $\varepsilon_1 = 0.1929 < \varepsilon$ and $\varepsilon_2 = 0.3185 > \varepsilon$. Thus, the initial matrix $\boldsymbol{P}^1$ can be obtained, as shown in (5). Matrix $\boldsymbol{P}^1$ indicates that the MCP$_{\mathrm{AA}}$ joints of the index finger, the ring finger and the little finger have low participation and could be removed.

$$\boldsymbol{P}^1 = \begin{bmatrix} 5.00 & 0 & 0 & 0 & 3.4 \\ 0 & 0 & 2.78 & 0 & 3.29 \\ 0 & 0 & 2.07 & 0 & 2.08 \\ 0 & 0 & 1.13 & 0 & 2.09 \\ 0 & 0 & 1.01 & 0 & 1.74 \end{bmatrix} \tag{5}$$

Subsequently, the variance and the maximum of the nonzero elements in matrix $\boldsymbol{P}^1$ are obtained, i.e., $D(\tilde{\mathrm{p}}_{ij}^1) = 1.44 > 1$ and $\max(\tilde{\mathrm{p}}_{ij}^1) = 5$, so $h = 1$. The variances of matrices with different coupling modes are also obtained, i.e., $D((\tilde{\mathrm{p}}_{ij}^1)_{L\to R}) = 1.06$, $D((\tilde{\mathrm{p}}_{ij}^2)_{M\to I}) = 3.28$, $D((\tilde{\mathrm{p}}_{ij}^2)_{L\to R,M\to I}) = 1.47$, $D((\tilde{\mathrm{p}}_{ij}^1)_{L\to R\to M}) = 1.39$, $D((\tilde{\mathrm{p}}_{ij}^1)_{L\to R\to M\to I}) = 6.29$, and $num(\min D((\tilde{\mathrm{p}}_{ij}^{r-1})_q) = 1$. Thus, the configuration that couples the MCP$_{\mathrm{FE}}$ joint of the little finger and the ring finger is an ideal result for the anthropomorphic hand that imitates the six basic human hand grasps. As a result, $\boldsymbol{P}_E$ equals to $\boldsymbol{P}_{L\to R}^1$, as shown in (6).

$$\boldsymbol{P}_E = \boldsymbol{P}_{L\to R}^1 = \begin{bmatrix} 5.00 & 0 & 0 & 0 & 3.40 \\ 0 & 0 & 2.78 & 0 & 3.29 \\ 0 & 0 & 2.07 & 0 & 2.08 \\ 0 & 0 & 2.14 & 0 & 3.83 \\ 0 & 0 & 0 & 0 & 0 \end{bmatrix} \tag{6}$$

After derving matrix $\boldsymbol{P}_E$, $(p_s^i)_E$ can be obtained by adding the participation of the same kind of motion (FE/AA) of each finger together, as shown in the left side of Table VII.

It can be seen from the result that $p_{FE}^T = 3.40$, $p_{AA}^T = 5.00$, $p_{FE}^M = 4.15$, $p_{FE}^I = 6.07$, $p_{FE}^R = 5.97$, and their average is $E((\tilde{p}_s^i)_E) = 4.92$, thus $\xi E((\tilde{p}_s^i)_E = 3.44$. Finally, $NOA\ ((p_s^i)_E)$ can be obtained by $INT((p_s^i)_E)/\xi E((\tilde{p}_s^i)_E)$. As shown in the right side of Table VII, $NOA((p_{FE}^T)_E) = 1$, $NOA(p_{AA}^T)_E) = 1$, $NOA((p_{FE}^I)_E) = 1$, $NOA((p_{FE}^M)_E) = 1$, and $NOA((p_{FE}^R)_E) = 1$. Therefore, p_{AA}^T, p_{FE}^T, p_{FE}^I, p_{FE}^M, and p_{FE}^R all can be realized by one actuator, respectively.

Therefore, the final simplified anthropomorphic hand configuration that imitates the six expected basic grasps of the human hand is obtained, as shown in Fig. 3(b). As a result, the AA and FE motions of the thumb are assigned to CMC joint and MCP joint respectively, and the rest of IP$_{\mathrm{FE}}$ joint is coupled; the FE motions of the index finger and the middle finger are each achieved by one actuator; the FE motion of the ring finger and the little finger are achieved by one actuator together. Therefore, the final configuration of the anthropomorphic hand has 5 active DOFs and 11 joints in all.

VI. Experiments Validation

A. Experimental Setup

To evaluate the simplified anthropomorphic hand configuration, a tendon-driven based hand called "CMIC-5" was developed to perform grasping test, as shown in Fig. 4(a). The dimension of the hand is 215 × 148 × 70 mm, which is about 1.2 times that of an adult male's hand. The structure and tendon-driven transmission of each finger has been optimized for meet the joint range of the human hand. As shown in Fig. 4(b), each MCP$_{\mathrm{FE}}$ joint of the index finger, the middle finger and the ring finger is driven by one motor respectively, and the MCP$_{\mathrm{FE}}$ motion of the little finger is coupled with ring finger

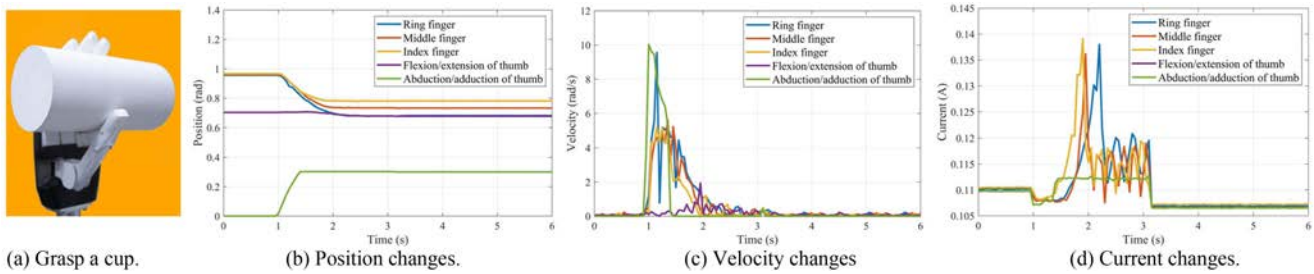

Fig. 5. A typical grasp test.

Fig. 6. Six basic human hand grasps experiments of the CMIC-5 hand. (a) grasping a cup; (b) grasping a drill; (c) grasping a strawberry, (d) grasping a ball, (e) grasping a bag, (f) grasping a pencil; (g) grasping a mouse; (h) grasping a key; (i) grasping a card.

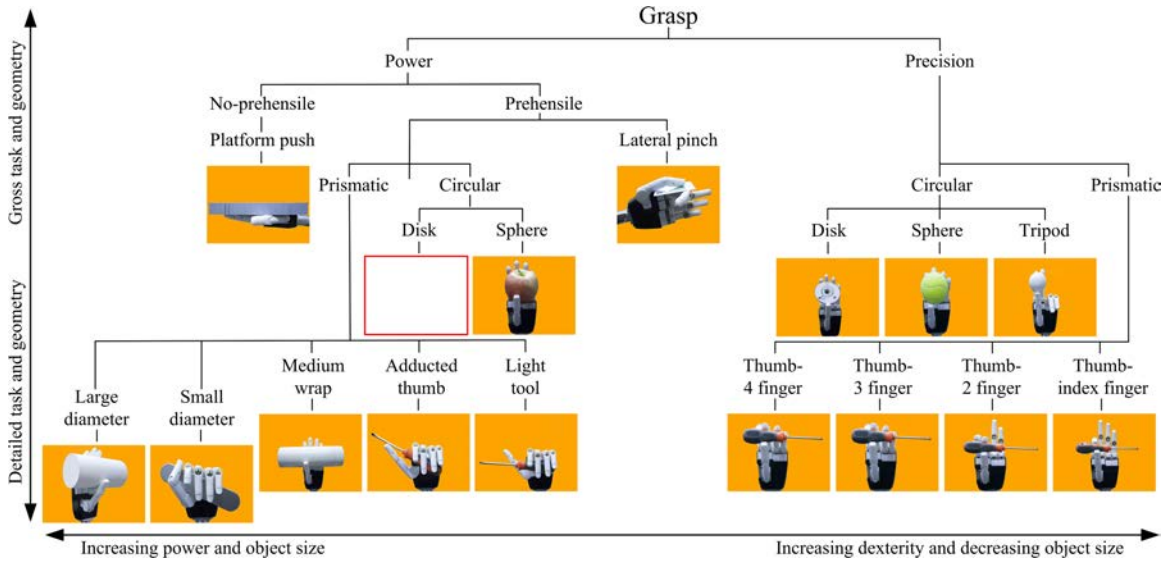

Fig. 7. Anthropomorphic grasps performed by CIMC-5 hand according to the Cutkosky taxonomy.

according to the simplified configuration. Meanwhile, each IP_{FE} joint of four fingers is coupled with its MCP_{FE} joint through a tendon-driven mechanism. The CMC_{AA} joint and MCP_{FE} joint of the thumb are driven by one motor respectively, and its IP_{FE} joint is also coupled with the MCP_{FE} joint through tendon-driven mechanism, as shown in Fig. 4(c). The motion transmission between the motor and CMC_{AA} or MCP_{FE} joint is realized by a fan-shaped worm gear to guarantee output torque while saving installation space. Thus, five actuators are used to drive 11 joints of the developed hand.

In order to verify the grasp performance of the CMIC-5 hand, a simple cup-grasping test was conducted, as shown in Fig. 5(a). The CMIC-5 hand was in the extended state pre-test, with the grasping action is executed from 1 s. It can be seen from Fig. 5(b) that the thumb mainly performed the adduction motion, while its flexion/extension motion is rarely involved. The other four fingers performed flexion motion, but the movement degrees are slightly different. Fig. 5(c) shows the velocity changes during the grasp. Before the hand contacts the cup, each motor moved at a uniform speed. At the moment of contact, the speed of each motor fluctuated slightly, but tended to zero quickly, indicating that the grasping had been successfully completed. Meanwhile, the current changes of each motor were also recorded, as shown in Fig. 5(d). The thumb contacted the cup first, then the index finger and the middle finger; finally, the ring finger and the little finger. This indicates that the movements of the four fingers during the grasp are different.

B. Six Human Hand Grasps Test

Experiments of six basic human hand grasps were conducted to verify the both gasp capability of the CMIC-5 hand and the simplified configuration design method. The initial hand posture before each grasp is set as Fig. 4(a), with all fingers and thumb fully extended. Fig. 6(a)–(i) show the cylindrical, tip, hook, palmar, spherical, and Lateral grasp, respectively. The results

show that the CMIC-5 hand can successfully perform the six expected human hand grasps.

C. Cutkosky Taxonomy Grasps Test

More grasp tests were conducted to evaluate the anthropomorphic grasping ability of the CMIC-5 hand. The Cutkosky taxonomy [24] is selected as the test paradigm, as it uses 16 different types of human hand grasps and is widely accepted to verify the function and dexterity of human and anthropomorphic hands. The test process was consistent with Section VI.B. Fig. 7 shows the performance of the CMIC-5 hand in realizing the Cutkosky taxonomy grasps.

It can be seen from the experimental results that the CMIC-5 hand performed all grasps successfully except for the disk grasp (power type) due to the absence of a large thenar structure in the palm. Note that due to the coupling of the little finger and the ring finger, the grasping effect of Thumb-3 finger is consistent with that of Thumb-4 finger. Consequently, the proposed simplified configuration design method can make an anthropomorphic hand with as few actuators as possible imitate expected human hand grasps, and can even perform some grasps beyond design considerations.

The development of an anthropomorphic hand imitating six basic human hand grasps is an illustrative example, and it is not the only possible application of the proposed method. The expected grasps can be got by measuring real human hand grasps or selected from classical human hand grasp taxonomy, such as the Cutkosky taxonomy and the Feix taxonomy [25].

VII. Conclusion

Aiming at the configuration design of an anthropomorphic hand imitating specific human hand grasps with as few actuators as possible, this letter presents a simplified configuration design method. The index "joint participation matrix" is proposed to characterize a human hand grasp from the joint level. Through mathematical transformations of the joint participation matrix corresponding to specific human hand grasps, joints or fingers that have the same joint participation and motion can be coupled to reduce the number of required actuators while ensuring grasp performance. Thus a simplified anthropomorphic hand configuration that imitates expected human hand grasps can be obtained. Taking the configuration design of an anthropomorphic hand imitating six basic human hand grasps as an example, a 5-DOFs anthropomorphic hand configuration was derived and a hand prototype CMIC-5 was developed for tests. A series of experiments demonstrated that the CMIC-5 hand can not only perform the six basic human hand grasps, but also 15 of 16 grasps of Cutkosky's taxonomy. Therefore, the proposed method can obtain the simplest configuration of an anthropomorphic hand when the expected human hand grasps are decided. In the next phase of research, further combinations involving static and dynamic grasps will be considered to verify the proposed method.

References

[1] C. Piazza, G. Grioli, M. G. Catalano, and A. Bicchi, "A century of robotic hands," *Annu. Rev. Control, Robot., Auton. Syst.*, vol. 2, pp. 1–32, May 2019.

[2] M. T. Mason and J. J. Kenneth Salisbury, *Robot Hands and the Mechanics of Manipulation*. Cambridge, MA, USA: MIT Press, 1985.

[3] J. Butterfass, M. Grebenstein, H. Liu, and G. Hirzinger, "DLR-hand II: Next generation of a dextrous robot hand," in *Proc. IEEE Int. Conf. Robot. Automat.*, 2001, vol. 1, pp. 109–114.

[4] "Shadow hand," [Online]. Available: http://www.shadowrobot.com

[5] "Schunk SVH hand," [Online]. Available: https://schunk.com

[6] R. Parent, "Modeling and animating human figures," in *Computer Animation*. New York, NY, USA: Springer, 2012, pp. 283–315.

[7] S. Arimoto, "Characterisations of human hands," in *Control Theory of Multi-Fingered Hands: A Modelling and Analytical-Mechanics Approach for Dexterity and Intelligence*. New York, NY, USA: Springer, 2008, pp. 1–39.

[8] C. Cipriani, M. Controzzi, and M. C. Carrozza, "Objectives, criteria and methods for the design of the smarthand transradial prosthesis," *Robotica*, vol. 28, no. 6, pp. 919–927, Dec. 2010.

[9] H. Liu, P. Meusel, G. Hirzinger, M. Jin, Y. Liu, and Z. Xie, "The modular multisensory DLR-HIT-hand: Hardware and software architecture," *IEEE/ASME Trans. Mechatronics*, vol. 13, no. 4, pp. 461–469, Aug. 2008.

[10] H. R. Wang, S. W. Fan, and H. Liu, "Thumb configuration and performance evaluation for dexterous robotic hand design," *J. Mech. Des.*, vol. 139, no. 1, Nov. 2017, Art. no. 012304.

[11] W. S. You et al., "Kinematic design optimization for anthropomorphic robot hand based on interactivity of finger," *Intell. Service Robot.*, vol. 12, no. 2, pp. 197–208, Feb. 2019.

[12] U. Kim et al., "Integrated linkage-driven dexterous anthropomorphic robotic hand," *Nature Commun.*, vol. 12, no. 1, pp. 1–13, Sep. 2021.

[13] S. H. Jeong, K.-S. Kim, and S. Kim, "Designing anthropomorphic robot hand with active dual-mode twisted string actuation mechanism and tiny tension sensors," *IEEE Robot. Automat. Lett.*, vol. 2, no. 3, pp. 1571–1578, Jul. 2017.

[14] M. Yin, D. Shang, T. Xu, and X. Wu, "Joint modeling and closed-loop control of a robotic hand driven by the tendon-sheath," *IEEE Robot. Automat. Lett.*, vol. 6, no. 4, pp. 7333–7340, Oct. 2021.

[15] C.-H. Xiong, W.-R. Chen, B.-Y. Sun, M.-J. Liu, S.-G. Yue, and W.-B. Chen, "Design and implementation of an anthropomorphic hand for replicating human grasping functions," *IEEE Trans. Robot.*, vol. 32, no. 3, pp. 652–671, Jun. 2016.

[16] S. B. Kang and K. Ikeuchi, "Grasp recognition using the contact web," in *Proc. IEEE/RSJ Int. Conf. Intell. Robots Syst.*, 1992, pp. 194–201.

[17] X. C. Liu and Q. Zhan, "Description of the human hand grasp using graph theory," *Med. Eng. Phys.*, vol. 35, no. 7, pp. 1020–1027, Jul. 2013.

[18] N. Palastanga and R. Soames, *Anatomy and Human Movement: Structure and Function*, 6th ed. Amsterdam, The Netherlands: Elsevier, 2012.

[19] A. I. Kapandji, *The Physiology of the Joints, Volume 1: Upper Limb*, 7th ed. Mountain View, CA, USA: Handspring, 2019.

[20] I. Komatsu and J. D. Lubahn, "Anatomy and biomechanics of the thumb carpometacarpal joint," *Operative Techn. Orthopaedics*, vol. 28, no. 1, pp. 1–5, Mar. 2017.

[21] C. D. Santina, C. Piazza, G. Grioli, M. G. Catalano, and A. Bicchi, "Toward dexterous manipulation with augmented adaptive synergies: The Pisa/IIT SoftHand 2," *IEEE Trans. Robot.*, vol. 34, no. 5, pp. 1141–1156, Oct. 2018.

[22] C. L. Taylor and R. J. Schwarz, "The anatomy and mechanics of the human hand," *Artif. Limbs*, vol. 2, no. 2, pp. 22–35, May 1955.

[23] Q. Zhan, C. Zhang, and Q. H. Xu, "Measurement and description of human hand movement," in *Proc. Int. Conf. Mech., Mater. Aerosp. Eng.*, 2017, Paper 04002.

[24] M. R. Cutkosky, "On grasp choice, grasp models, and the design of hands for manufacturing tasks," *IEEE Trans. Robot. Automat.*, vol. 5. no. 3, pp. 269–279, Jun. 1989.

[25] T. Feix, J. Romero, H.-B. Schmiedmayer, A. M. Dollar, and D. Kragic, "The grasp taxonomy of human grasp types," *IEEE Trans. Hum.-Mach. Syst.*, vol. 46, no. 1, pp. 66–77, Feb. 2016.